Journal of Biomolecular NMR, 9 (1997) 389–395

J-Bio NMR 435

The effect of ring currents on carbon chemical shifts in cytochromes

Laurence Blanchard, C. Neil Hunter and Michael P. Williamson*

Krebs Institute, Department of Molecular Biology and Biotechnology, University of Sheffield, Firth Court, Western Bank, Sheffield S10 2TN, U.K.

Received 28 October 1996
Accepted 15 February 1997

Keywords: Carbon chemical shifts; Cytochrome c; Secondary structure; Heme ring current effect

Summary

Calculations suggest that some carbon chemical shifts in proteins should have large ring current shifts (>1 ppm). We present ^{13}C, ^{15}N and ^{1}H assignments for cytochrome c_2 from *Rhodospirillum rubrum*, compare these with shifts for other cytochromes c, and show that the calculated ring current shifts are similar to experimentally observed shifts, but that there remain substantial conformation-dependent shifts of side-chain carbons. Ring current shifts as large as 6 ppm are observed. We show that the ring current effects do not seriously affect the Chemical Shift Index method for delineating secondary structure, but may have an impact on more precise methods for generating structural constraints.

Introduction

Chemical shifts have been used as a tool (albeit a very blunt one) to aid protein structure determination since the very first observations of protein NMR spectra (Saunders et al., 1957). With the advent of complete assignments of proteins of known structure, it has become possible to develop reasonably good predictive methods for calculation of ^{1}H shifts from the known structure (Ösapay and Case, 1991; Williamson et al., 1992; Szilágyi, 1995). These methods are based on well-established equations that were developed using organic molecules, such as the Haigh–Mallion or Johnson–Bovey methods for calculating ring current shifts (Johnson and Bovey, 1958; Haigh and Mallion, 1972). More recently, as experimental ^{13}C shift assignments have become available, both empirical (Spera and Bax, 1991; Wishart and Sykes, 1994a) and theoretical (de Dios et al., 1993a,b) methods have been developed for calculating ^{13}C shifts. ^{13}C shifts are now widely used to provide initial constraints for protein structure determination, through the Chemical Shift Index (CSI) (Wishart et al., 1991,1992; Wishart and Sykes, 1994b). This is based on the empirical observation that C^{α}, C^{β} and C' shifts in proteins have a dependence on local secondary structure. A number of groups are now trying to extend this idea and generate more precise constraints, by using the dependence of the C^{α} and C^{β} shift on the ϕ,ψ angle to put more precise constraints on the backbone dihedral angles (Celda et al., 1995; Kuszewski et al., 1995; Pearson et al., 1995).

Methods such as those of Haigh–Mallion or Johnson–Bovey for calculating ^{1}H chemical shifts arising from aromatic ring currents are expected to be equally applicable to ^{13}C shifts, with the chemical shift effect for ^{13}C being equal in ppm to the effect for a ^{1}H nucleus at the same position. They are therefore expected to be reasonably large, and can easily be >1 ppm. Particularly large effects are expected in proteins containing heme rings, since heme rings produce large ring current shifts. In this paper we present the chemical shift assignment for cytochrome c_2 from *Rhodospirillum rubrum*, present the differences in chemical shifts from the expected random coil values, and compare these to calculated shifts. We examine the effect that ring current shifts have on both the CSI and the more precise methods for structure calculation. This cytochrome is particularly suitable for such a study, since it has a very high resolution crystal structure (Salemme et al., 1973).

*To whom correspondence should be addressed.

Experimental methods

Protein preparation

Rhodospirillum rubrum cytochrome c_2 uniformly labelled with ^{13}C and ^{15}N was prepared by growing 6 l of *Rhodospirillum rubrum* S1 in M22 minimal medium containing $^{13}C_2$ sodium acetate (2 g/l, Isotec Inc., Veenendaal, The Netherlands) and $^{13}C_6$ glucose (0.5 g/l, Promochem, Welwyn Garden City, U.K.) as the sole carbon sources, and $(^{15}NH_4)_2SO_4$ (0.5 g/l, Isotec Inc.) as the sole nitrogen source, under photosynthetic growth conditions at 34 °C. Cells were harvested by centrifugation in late-log phase. Periplasmic proteins were obtained by incubation of the cells in 0.05 M Tris-HCl, pH 9.0 and 0.05 M EDTA, 30 min at 37 °C. The mixture was centrifuged (13 000 × g, 1 h, 4 °C). The supernatant was then dialysed overnight against water and applied to an anion exchange column (DE-52, Whatman (Maidstone, U.K.), 2.5 cm × 20 cm) equilibrated with 10 mM Tris-HCl, pH 8.0. The cytochrome fraction was eluted with a gradient 30–90 mM Tris-HCl, pH 8.0 and found in the 50 mM Tris-HCl fraction, then loaded onto a hydroxyapatite column (Biorad (Hemel Hempstead, U.K.), Biogel HTP, 2.5 cm × 5 cm) equilibrated with 50 mM Tris-HCl, pH 8.0. Two cytochrome-containing fractions were eluted: cytochrome c_2 with 50 mM potassium phosphate buffer, pH 8.0 and cytochrome c' with 1 M potassium phosphate buffer, pH 8.0. *Rhodospirillum rubrum* cytochrome c_2 (6.4 mg) was obtained and estimated to be pure by SDS-PAGE and from the purity coefficient (Bartsch, 1971)

$$[OD_{272red}/OD_{415red}] = 0.23$$

The NMR sample was prepared in potassium phosphate buffer (50 mM, pH 5.7) with 90% H_2O/10% D_2O at a protein concentration of 1.8 mM (6.4 mg in 275 µl in a Shigemi 5 mm tube). Full reduction of the sample was obtained by the addition of 4 mol/mol disodium dithionite in 0.1 M potassium phosphate buffer at pH 8.0 under argon atmosphere.

NMR experiments

The spectra were acquired on Bruker AMX-500 and DRX-500 spectrometers at 308 K. Quadrature detection in the indirectly detected dimensions was obtained for the ^1H-^{15}N HSQC (heteronuclear single quantum coherence) experiment by phase cycling the appropriate pulses according to the time-proportional phase incrementation method (TPPI; Marion and Wüthrich, 1983) and for the other experiments by the States-TPPI (Marion et al., 1989b) method. The H_2O signal was suppressed by low-power presaturation during the recycling delay except for the HC(C)H-TOCSY, for which pulsed-field gradients were used (Kay, 1995). ^1H chemical shifts were referenced to the H_2O resonance which had been calibrated independently at 4.69 ppm (308 K) relative to sodium 3-trimethylsilyl-2,2,3,3-($^2H_4$)propionate. ^{15}N and ^{13}C chemical shifts were referenced indirectly by using the above ^1H frequencies for the H_2O resonance and the ratios of gyromagnetic ratios given in Wishart et al. (1995).

Three 2D experiments (^1H-^{15}N HSQC, ^1H-^{13}C HSQC, 2D HN(CA)CO) and six triple-resonance experiments (HNCA, HNCO (Kay et al., 1990; Bax and Ikura, 1991), HN(CO)CA (Grzesiek and Bax, 1992a), CBCA(CO)NH (Grzesiek and Bax, 1992b), HBHA(CBCACO)NH (Grzesiek and Bax, 1993) and HC(C)H-TOCSY (Kay et al., 1993)) were used. For the triple-resonance experiments the following numbers of complex points were employed: H^N 512 or 1024, ^{15}N 32, $^{13}C^\alpha$ 56, $^{13}C^\alpha/^{13}C^\beta$ 40 and ^1H 110. Typical spectral widths were 6250 Hz, 1524 Hz, 3521 Hz and 2645 Hz for ^1H, ^{15}N, $^{13}C^\alpha$ and $^{13}C'$, respectively.

NMR data were processed on Silicon Graphics workstations using FELIX version 95.0 (Biosym Technologies Inc., San Diego, CA, U.S.A.). Spectra were typically zero-filled to 1024 points over 6250 Hz in the acquisition dimension, and in the indirect dimensions to 256 points (^1H), 64 or 128 points (^{13}C), and 64 or 128 points (^{15}N), and processed with a 60°- or 70°-shifted sine-bell function in all dimensions. Residual solvent resonances were removed by applying a time domain convolution filter as described by Marion et al. (1989a).

The backbone resonances were assigned using the 3D spectra HNCA, HN(CO)CA, HNCO and the 2D HN(CA)CO in conjunction with the 2D ^1H-^{15}N HSQC spectrum, followed by the side-chain resonance assignment

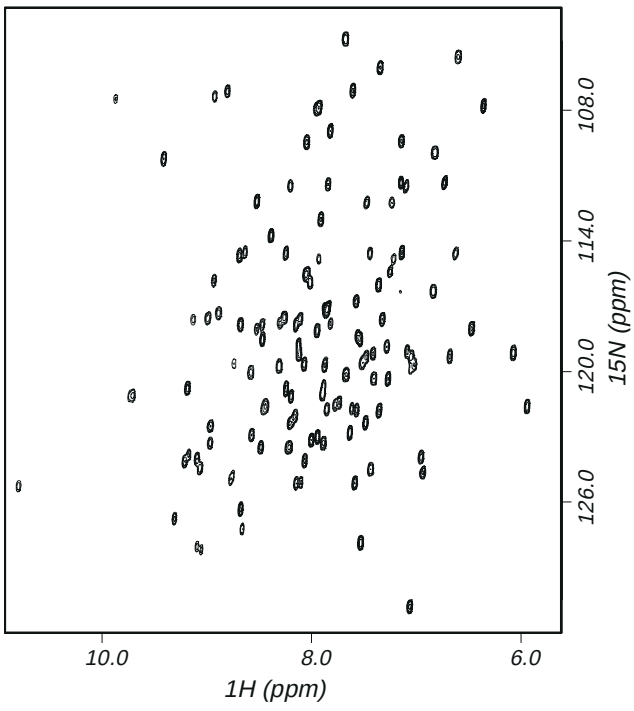

Fig. 1. 2D ^1H-^{15}N HSQC spectrum of uniformly $^{13}C/^{15}N$-labelled *Rhodospirillum rubrum* cytochrome c_2.

using the CBCA(CO)NH, HBHA(CBCACO)NH and HC(C)H-TOCSY. The spectra were analysed using locally written programs for matching chemical shift values. The 2D ^{1}H-^{13}C HSQC was used to assign the methionine ligand ^{13}C side-chain resonances using the ^{1}H chemical shift resonances of axial ligands assigned previously (Yu and Smith, 1990).

Calculations

^{13}C chemical shifts were calculated using the Haigh–Mallion method (Haigh and Mallion, 1972), with ring current intensity factors optimised for ^{1}H shifts in proteins. Intensity factors for the heme ring were taken from Ösapay and Case (1991), while all others were taken from Williamson et al. (1992). The program can be obtained from http://www.shef.ac.uk/~mbb/nmr/home.html and is identical to the ring current shift part of the ^{1}H shift calculation program which has been used successfully on a wide range of proteins and can be found in the same source (Williamson et al., 1992). The Brookhaven Protein Databank entry codes used were 3C2C, 1C2R and 1HRC for *Rhodospirillum rubrum* cytochrome c_2, *Rhodobacter capsulatus* cytochrome c_2 and horse cytochrome c, respectively. The CSI implementation was obtained via ftp at the following address: canopus.biochem.ualberta.ca from Wishart and Sykes (1994b).

Results and Discussion

The ^{1}H, ^{15}N and ^{13}C assignment of the reduced cytochrome c_2 from *Rhodospirillum rubrum* was made using a combination of 2D and 3D methods. Almost all signals are resolved in the ^{1}H-^{15}N HSQC spectrum (Fig. 1). The assignments are given in Table 1. Some signals were found to be split into two; these are localised to two segments of the chain that are adjacent in the three-dimensional structure, and form the interface between the N- and C-terminal helices. Such a doubling of signals from the N- and C-terminal helices in cytochromes c has been seen previously by Chau et al. (1990) and Blanchard et al. (1996). In this study, we have used the more intense set of signals for subsequent characterisations.

The ^{13}C chemical shifts are in general close to their random coil values, particularly for side-chain atoms. Some major deviations were seen, particularly in His^{18} and Met^{91}, which form the heme axial ligands and are therefore situated directly over and under the heme ring. The C^{β}, C^{γ} and C^{ε} carbons of Met^{91} have shifts 5.7, 3.3 and 1.6 ppm upfield, respectively, from their expected random coil positions.

In order to check that calculations based on the standard methods used for ^{1}H are valid for ^{13}C, we have calculated the chemical shift changes due to ring current shifts (from the heme and from other aromatic rings) for all carbon atoms, in exactly the same way as we calculate them for protons. The calculated shifts for backbone carbons (C^{α}, C^{β}, C') are affected by the local secondary structure (Spera and Bax, 1991; Wishart and Sykes, 1994a), so for this comparison we have concentrated on side-chain atoms. Comparisons of calculated shifts and experimental differences from random coil shifts are shown in Fig. 2 for *Rhodospirillum rubrum* cytochrome c_2, and also for *Rhodobacter capsulatus* cytochrome c_2 and horse cytochrome c. The correlation coefficient between calculated and observed shift differences is 0.25, showing a weak correlation. We conclude that it is justifiable to use the same methods for calculating ^{13}C ring current shifts as for ^{1}H ring current shifts, but that ^{13}C shifts, even of side-chain carbons, have large additional conformation-dependent shifts that are still poorly understood. The origin of these effects may lie in perturbation of p-orbital electron density caused by steric or electronic interactions from neighbouring groups, essentially the phenomenon previously described as the γ-effect (Grant and Paul, 1964).

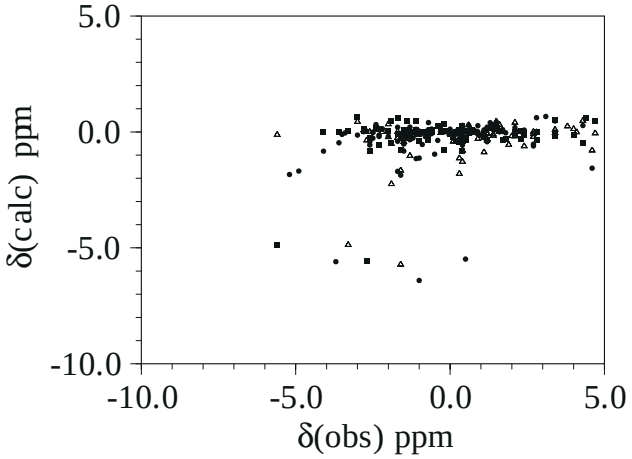

Fig. 2. Comparison of calculated shifts and experimental differences from random coil shifts for carbon side-chain atoms from *Rhodospirillum rubrum* cytochrome c_2 (Δ), *Rhodobacter capsulatus* cytochrome c_2 (●) and horse cytochrome c (■). The carbon shifts for *Rhodobacter capsulatus* cytochrome c_2 and horse cytochrome c were obtained from Caffrey et al. (1994) and Gao et al. (1990), respectively. The carbon atoms with large calculated secondary shifts are all from the methionine axial heme ligands, except for the *Rhodobacter capsulatus* carbon with a calculated shift of –6.4 ppm, which is from the axial histidine Cε1.

The calculations suggest that a large number of carbon atoms will have large chemical shift effects from aromatic rings (particularly from the heme). In *Rhodospirillum rubrum* cytochrome c_2, 29 atoms out of 529 are calculated to have ring current shifts of >1 ppm. It is therefore possible that methods that use ^{13}C shifts for structural constraints will be adversely affected by the ring current shifts. We have used the CSI (Wishart and Sykes, 1994b) to characterise the secondary structure of the protein. This method can use $^{1}H^{\alpha}$, $^{13}C^{\alpha}$, $^{13}C^{\beta}$ and ^{13}C' shifts simultaneously for the characterisation. In this study we used

TABLE 1
CHEMICAL SHIFTS OF ^{1}H, ^{15}N AND ^{13}C NUCLEI IN CYTOCHROME c_2 FROM *RHODOSPIRILLUM RUBRUM* AT 308 K

Residue	^{15}N (H^N) (ppm)	C' (ppm)	C^α (H^α) (ppm)	C^β (H^β) (ppm)	Others (ppm)
E1	107.5 (9.87)	178.4	48.3		
G2		168.3	43.5 (4.25, 3.56)		
D3[a]	121.7 (8.45)	175.7	52.6 (4.90)	43.4 (2.66)	
A4[a]	128.1 (9.09)	179.0	55.6 (3.96)	17.8 (1.47)	
A5	122.4 (8.21)	181.3	55.0 (4.30)	16.5 (1.54)	
A6	123.0 (7.94)	182.3	54.7 (4.18)	17.1 (1.49)	
G7[a]	107.4 (8.93)	174.7	46.8 (4.16, 3.40)		
E8[a]	125.2 (8.15)	180.0	58.8 (2.41)	28.5 (1.99, 1.69)	C^γ 35.4 (1.80)
K9	119.4 (7.05)	180.3	59.9 (4.06)	31.7 (2.03)	C^γ 25.0 (1.61, 1.43); C^δ 29.2 (1.70); C^ε 42.2 (3.00)
V10	121.4 (7.74)	178.2	66.4 (3.82)	31.7 (2.30)	C^γ 22.8 (1.33); C^γ 22.4 (1.26)
S11	114.6 (8.25)	175.0	61.9 (3.57)	62.2	
K12	121.8 (7.36)	180.4	58.8 (4.16)	31.5 (2.03)	C^δ 28.6 (1.70); C^ε 42.2 (2.98)
K13	117.9 (8.68)	178.3	59.6 (4.37)	33.5 (2.36)	C^ε 42.5 (3.30)
C14	115.6 (8.05)	177.7	54.9 (5.17)	34.6 (2.98, 2.59)	
L15	118.4 (7.56)	176.7	55.9 (4.47)	42.3 (1.91, 1.61)	C^δ 25.8 (0.95); C^δ 23.4 (0.87)
A16	119.2 (7.41)	178.5	54.8 (4.14)	17.7 (1.69)	
C17	110.0 (6.82)	172.0	53.7 (4.37)	40.5 (1.87, 0.72)	
H18	116.3 (6.84)	173.0	53.2 (3.33)	30.9 (0.44)	
T19	105.5 (6.60)	173.7	59.2 (4.02)	71.7 (4.37)	C^γ 21.5 (1.00)
F20	117.3 (8.89)	174.0	58.6 (4.28)	29.4 (2.32)	
D21	114.7 (8.69)	177.7	52.9 (4.52)	40.4 (2.64, 2.28)	
Q22	126.3 (8.68)	176.9	58.1 (3.15)	26.5 (1.33, 0.11)	C^γ 33.4 (1.74, 1.58)
G23	117.6 (9.13)	175.0	45.1 (3.93, 3.59)		
G24	107.1 (7.61)	172.8	44.7 (3.83, 3.45)		
A25	120.8 (8.24)	179.5	51.7 (4.11)	18.7 (1.23)	
N26	119.7 (8.74)	174.3	53.1 (4.20)	38.7 (2.39, 2.75)	
K27	124.5 (7.44)	175.4	55.4 (4.36)	31.7 (1.59, 1.14)	C^ε 41.5 (2.54)
V28	123.9 (6.95)	177.4	66.2 (3.94)	33.5 (1.91)	C^γ 21.1 (1.65); C^γ 22.4 (1.31)
G29	104.7 (7.68)		41.5		
P30		176.2	59.9 (3.47)	31.5 (1.32, 0.91)	
N31	120.7 (7.89)	175.0	54.7 (3.89)	41.0 (2.24, 1.63)	
L32	119.6 (7.51)	175.4	53.5 (3.87)	42.6 (1.19, 0.67)	C^γ 24.4 (–0.35); C^δ 21.1 (–0.69); C^δ 23.4 (–2.24)
F33	119.1 (7.09)		61.9		
G34		174.6	46.3 (3.90, 3.78)		
V35	119.4 (7.48)	174.5	64.2 (3.31)	32.0 (1.55)	C^γ 20.5 (0.97); C^γ 23.7 (0.78)
F36	123.3 (8.97)	175.4	60.8 (3.92)	39.3 (2.96, 2.60)	
E37	121.6 (8.44)	173.3	59.2 (2.88)	26.5 (2.08, 1.79)	C^γ 37.7 (1.47, 1.13)
N38	119.8 (8.31)	174.7	50.3 (4.97)	40.4 (3.15, 2.84)	
T39	110.2 (9.41)	175.4	62.0 (4.51)	71.8	C^γ 28.8 (1.30)
A40	119.3 (6.68)	179.2	53.0 (4.69)	19.4 (1.27)	
A41	125.3 (10.74)	178.4	51.6 (2.61)	15.4 (0.99)	
H42	115.8 (8.93)	174.1	59.3 (4.19)	27.6 (–0.73)	
K43	121.8 (7.86)	176.3	54.0 (4.28)	34.2 (0.46)	C^ε 42.2 (3.19)
D44	127.3 (8.67)	176.1	57.2 (4.54)	40.7 (2.84)	
N45	115.9 (8.02)	174.9	52.3 (4.67)	39.6 (3.02, 2.52)	
Y46	120.3 (7.41)	173.3	57.0 (4.35)	40.5 (2.66, 2.30)	
A47	130.8 (7.06)	174.5	50.4 (4.51)	15.3 (1.06)	
Y48	124.1 (8.07)		59.2		
S49		176.3	62.0 (4.69)	63.5 (4.30)	
E50	126.8 (9.31)	177.6	60.2 (4.24)	41.8 (3.43, 2.52)	
S51	114.5 (8.64)	177.2	60.7 (4.53)	63.1 (4.15, 3.76)	
Y52	122.9 (8.57)	178.0	62.4 (4.44)	37.9 (3.62, 2.98)	
T53	116.8 (7.57)	179.3	66.1 (3.96)	68.2 (4.54)	C^γ 22.8 (1.39)
E54	123.5 (8.48)	177.9	59.3 (4.23)	28.8 (2.46, 2.05)	C^γ 35.1 (2.65, 2.39)
M55	117.6 (8.11)	180.4	60.5 (3.81)	33.2 (2.35, 1.63)	
K56	121.2 (8.20)	179.2	60.3 (3.87)	31.9 (2.07)	C^ε 42.5 (3.08)
A57	123.2 (8.00)	176.9	54.7 (4.24)	16.8 (1.61)	
K58	116.0 (7.36)		56.5 (4.34)	32.6 (2.10, 1.79)	C^γ 25.1 (1.65, 1.48); C^δ 29.2 (1.61); C^ε 42.2 (2.99, 2.91)
G59	107.8 (7.93)	174.4	45.5 (4.15, 3.72)		

TABLE 1
(continued)

Residue	^{15}N (H^N) (ppm)	C' (ppm)	C^α (H^α) (ppm)	C^β (H^β) (ppm)	Others (ppm)
L60	122.4 (7.49)	176.7	57.7 (3.94)	41.7 (1.49, 1.37)	C^δ 25.7 (0.59); C^δ 23.4 (0.08)
T61	117.0 (7.87)	175.1	58.6 (3.68)	72.7 (4.76)	C^γ 21.5 (0.92)
W62	124.1 (9.09)	177.3	54.5 (5.31)	27.6 (3.58, 3.23)	
T63	113.0 (7.91)	175.3	60.9 (4.24)	71.4 (4.85)	C^γ 22.1 (1.31)
E64	121.1 (9.71)	178.3	61.7 (4.15)	29.4 (2.33)	C^γ 37.0 (2.65, 2.43)
A65	118.5 (8.47)	181.3	55.1	17.5	
N66	117.3 (7.86)	177.7	55.5 (5.06)	37.7 (3.33, 2.95)	
L67	120.8 (9.18)	177.9	58.9 (4.12)	43.4 (2.32, 1.37)	C^δ 27.3 (1.24); C^δ 23.4 (0.86)
A68	119.3 (8.12)	178.8	55.3 (3.90)	17.1 (1.42)	
A69	117.6 (7.32)	179.5	54.3 (4.10)	17.6 (1.75)	
Y70	119.7 (8.07)	176.1	61.3 (3.23)	39.2 (2.48, 1.70)	
V71	108.9 (7.82)	175.2	63.8 (2.51)	31.4 (1.81)	C^γ 21.0 (0.96); C^γ 21.7 (0.85)
K72	118.0 (6.47)	177.3	57.5 (4.37)	33.4 (1.69)	C^γ 25.4 (1.52, 1.35); C^d 29.6 (1.61); C^ε 42.2 (2.87)
D73	107.8 (6.36)		53.2		
P74		178.0	65.6 (3.42)	32.0 (1.07, 0.69)	C^γ 26.3 (0.61, –0.21); C^δ 50.3 (3.00, 2.78)
K75	114.5 (7.14)	178.0	59.2 (3.70)	32.0 (1.75)	C^ε42.5 (2.56, 2.43)
A76	120.3 (7.27)	180.6	54.3 (3.99)	17.3 (1.30)	
F77	118.8 (8.12)	177.4	61.9 (4.14)	40.5 (3.23)	
V78	112.2 (8.52)	180.0	65.1 (4.25)	31.4 (2.03)	C^γ 21.1 (1.04); C^γ 19.2 (0.96)
L79	125.1 (7.59)	178.2	58.9 (3.91)	42.8 (1.76, 1.56)	C^δ 24.7 (0.96); C^δ 25.7 (0.87)
E80	118.5 (7.53)	179.3	59.0 (3.91)	29.7 (2.02, 1.84)	
K81	113.8 (8.39)	178.9	55.9 (3.98)	31.9 (1.44, 1.20)	
S82	111.4 (7.84)	175.3	60.9 (3.86)	64.6	
G83	109.4 (7.14)	172.3	46.2 (3.94, 3.76)		
D84	121.1 (7.90)		49.6		
P85		177.6	64.0 (4.34)	32.3 (2.37, 1.98)	C^γ 27.0 (2.04, 1.96); C^δ 50.9 (4.00)
K86	117.5 (8.26)	176.0	55.0 (4.39)	31.4 (2.02, 1.76)	C^γ 25.2 (1.39); C^ε42.1 (3.04)
A87	122.8 (7.63)	177.2	53.6 (4.07)	19.6 (1.44)	
K88	120.1 (8.58)	175.4	54.2 (4.68)	37.1 (1.89)	C^δ 29.2 (1.74); C^ε 42.2 (3.07)
S89	109.5 (8.05)		57.1		
K90		176.3	57.1 (4.49)	33.1 (2.48, 2.33)	C^γ 26.0 (1.77); C^δ 29.6 (2.12, 2.04); C^ε 42.5 (3.52, 3.34)
M91	122.1 (8.16)	173.0	55.9 (3.29)	26.9 (0.03, –2.60)	C^γ 28.6 (–3.58, –1.21); C^ε 15.1 (–2.90)
T92	118.9 (7.28)	173.3	60.2 (3.84)	67.4 (4.46)	C^γ 20.5 (1.17)
F93	121.6 (5.94)	170.5	57.6 (4.15)	42.6 (3.17, 1.30)	
K94	119.2 (6.08)	174.0	53.6 (3.91)	34.9 (1.32, 1.12)	C^γ 23.1 (0.83, 0.70); C^δ 29.2 (1.48, 1.35); C^ε 42.2 (2.69)
L95	120.1 (7.67)	175.5	53.1 (4.40)	45.3 (1.48, 1.24)	
T96	108.0 (7.94)	175.1	62.0 (4.33)	70.0 (4.26)	C^γ 20.5 (1.02)
K97	123.3 (7.89)	177.1	55.8 (4.57)	33.3 (2.19, 1.75)	C^ε 42.2 (3.08)
D98	124.9 (8.77)	177.8	58.3 (4.32)	40.7 (2.68)	
D99	117.6 (8.99)	177.8	56.6 (4.39)	39.1 (2.51, 2.69)	
E100[a]	119.7 (7.02)	178.8	60.0 (4.18)	29.4 (2.28)	
I101	119.7 (7.88)	177.1	66.0 (3.55)	38.5 (2.00)	$C^{\gamma 1}$ 30.1 (1.74, 0.70); $C^{\gamma 2}$ 17.6 (0.90); C^δ 13.4 (0.70)
E102	117.9 (8.15)	180.4	59.6 (3.97)	29.3 (2.08)	
N103[a]	117.9 (8.47)	177.5	56.1 (4.56)	36.6 (2.91, 2.58)	
V104[a]	123.9 (9.18)	177.6	66.5 (4.13)	31.1 (2.50)	C^γ 20.5 (1.47); C^γ 24.1 (1.43)
I105	123.5 (8.22)	176.5	66.8 (3.71)	37.5 (2.03)	C^δ 14.7 (1.02)
A106[a]	121.8 (7.57)	180.4	55.4	16.0	
Y107	117.0 (7.84)	178.3	60.7 (4.36)	37.9 (3.45, 3.08)	
L108	122.5 (8.97)	179.7	58.2 (3.65)	41.5 (2.25, 1.29)	C^γ 26.6 (2.35); C^δ 23.1 (1.00)
K109	118.1 (7.95)	176.7	59.5 (3.23)	32.4 (1.38)	C^γ 23.7 (0.96, –0.30); C^δ 29.9 (1.31); C^ε 41.9 (2.69, 2.59)
T110	106.0 (7.35)	175.3	62.5 (4.27)	70.2 (4.34)	C^γ 21.1 (1.35)
L111	124.7 (6.94)	174.0	52.5 (4.35)	39.3 (1.74, 0.99)	C^δ 21.5 (0.66)
K112	127.9 (7.53)		56.9		

[a] Residues which present a duplication of their resonances.

only the $^{13}C^\alpha$, $^{13}C^\beta$ and $^{13}C'$ shifts because the $^1H^\alpha$ shifts have some very significant ring current effects and are therefore likely to be less reliable. The results are presented in Fig. 3, together with the true secondary structure as determined in the crystal structure using the Kabsch and Sander algorithm (Kabsch and Sander, 1983). We are

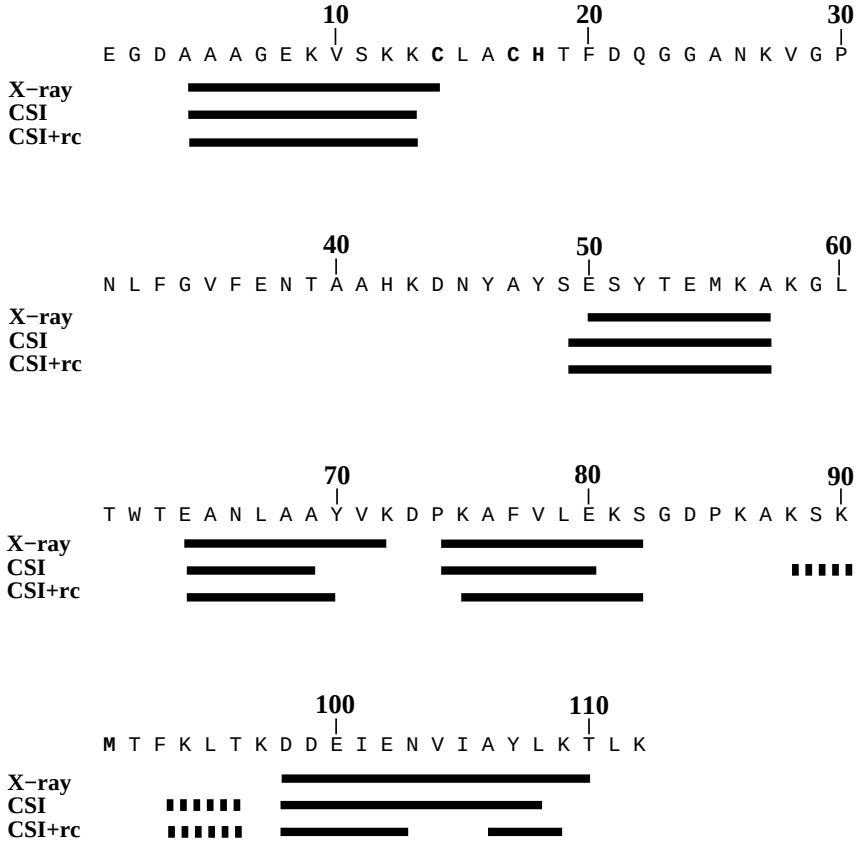

Fig. 3. Secondary structure of *Rs. rubrum* cytochrome c_2. Below the sequence, the bars indicate the secondary structure in the crystal structure (X-ray), the secondary structure predicted by the CSI (CSI), and the secondary structure predicted by the CSI after subtraction of calculated ring current effects (CSI + rc). Solid bars indicate helices and dotted lines indicate β-sheet. Residues predicted as coil are left blank. Heme ligands are given in bold type.

currently engaged in calculating the solution structure from our data, but preliminary studies indicate that solution and crystal structures are very similar. Any differences between the CSI-predicted and crystal secondary structures are therefore likely to be due to inaccuracies in the CSI method, possibly arising from ring current shifts.

The results presented in Fig. 3 indicate that the CSI is not strongly affected by ring current shifts. In order to estimate how ring current shifts perturb the CSI, we have calculated ring current shifts for all carbons based on the crystal structure, subtracted these from the experimental shifts and recalculated the secondary structure from the CSI (bottom line of Fig. 3). There is very little difference. The most obvious change is that a short stretch (residues 88–90) mistakenly predicted as being β-sheet in the original calculation is now correctly predicted as coil. Met^{91} is one of the two axial heme ligands, so this region is close to the heme. The reliability of the CSI, even in the presence of large individual ring current shifts, arises from the averaging used in the calculation of secondary structure from the index: if one or two carbon shifts are strongly perturbed, this is usually not enough to invalidate the method.

The situation is not as good for methods that use individual ^{13}C shifts directly as structure constraints. We calculate that nine C^{α} or C^{β} atoms have ring current shifts of 1 ppm or greater and 27 of 0.5 ppm or greater. Because of the shape of the ϕ,ψ surface (Spera and Bax, 1991) this means that they will typically be constrained to an angle 40° in error. This is clearly undesirable, and implies that individual ^{13}C shifts may be better used only in the final stages of a structure refinement, when it would be possible to include ^{13}C ring current shifts in the calculation. We note, however, that significant ^{13}C ring current effects are rarer in non-heme proteins: in a range of 'normal' proteins, the proportion of C^{α} and C^{β} atoms with calculated ring current shifts of >1 ppm is 0.7% and of >0.5 ppm it is 4%.

Conclusions

In *Rhodospirillum rubrum* cytochrome c_2, ring current shifts as large as 5.7 ppm have been observed. However, in typical non-heme proteins only about 0.7% of the C^{α} and C^{β} have calculated ring current shifts of >1 ppm. This has no significant impact on the CSI method, but may introduce errors into methods that directly use ^{13}C chemical shifts as structural constraints.

Acknowledgements

We are greatly indebted to Dr. Jeremy Craven (Sheffield) for his assistance with the programs for assignment and to Dr. Glyn Williams (Roche) for allowing us spectrometer time.

References

Bartsch, R.G. (1971) *Methods Enzymol.*, **23**, 344–363.

Bax, A. and Ikura, M. (1991) *J. Biomol. NMR*, **1**, 99–104.

Blanchard, L., Blackledge, M., Marion, D. and Guerlesquin, F. (1996) *FEBS Lett.*, **389**, 203–209.

Caffrey, M., Brutscher, B., Simorre, J.-P., Fitch, J., Cusanovich, M. and Marion, D. (1994) *Eur. J. Biochem.*, **221**, 63–75.

Celda, B., Biamonti, C., Arnau, M.J., Tejero, R. and Montelione, G.T. (1995) *J. Biomol. NMR*, **5**, 161–172.

Chau, M., Cai, M. and Timkovich, R. (1990) *Biochemistry*, **29**, 5076–5087.

de Dios, A.C., Pearson, J.G. and Oldfield, E. (1993a) *Science*, **260**, 1491–1496.

de Dios, A.C., Pearson, J.G. and Oldfield, E. (1993b) *J. Am. Chem. Soc.*, **115**, 9768–9773.

Gao, Y., Boyd, J. and Williams, R.J.P. (1990) *Eur. J. Biochem.*, **194**, 355–365.

Grant, D.M. and Paul, E.G. (1964) *J. Am. Chem. Soc.*, **86**, 2984–2990.

Grzesiek, S. and Bax, A. (1992a) *J. Magn. Reson.*, **96**, 432–440.

Grzesiek, S. and Bax, A. (1992b) *J. Am. Chem. Soc.*, **114**, 6291–6293.

Grzesiek, S. and Bax, A. (1993) *J. Biomol. NMR*, **3**, 185–204.

Haigh, C.W. and Mallion, R.B. (1972) *Org. Magn. Reson.*, **4**, 203–228.

Johnson, C.E. and Bovey, F.A. (1958) *J. Chem. Phys.*, **29**, 1012–1014.

Kabsch, W. and Sander, C. (1983) *Biopolymers*, **22**, 2577–2637.

Kay, L.E., Ikura, M., Tschudin, R. and Bax, A. (1990) *J. Magn. Reson.*, **89**, 496–514.

Kay, L.E., Xu, G.-Y., Singer, A.U., Muhandiram, D.R. and Forman-Kay, J.D. (1993) *J. Magn. Reson.*, **B101**, 333–337.

Kay, L.E. (1995) *Curr. Opin. Struct. Biol.*, **5**, 674–681.

Kuszewski, J., Qin, J., Gronenborn, A.M. and Clore, G.M. (1995) *J. Magn. Reson.*, **B106**, 82–96.

Marion, D. and Wüthrich, K. (1983) *Biochem. Biophys. Res. Commun.*, **113**, 967–974.

Marion, D., Ikura, M. and Bax, A. (1989a) *J. Magn. Reson.*, **84**, 425–430.

Marion, D., Ikura, M., Tschudin, R. and Bax, A. (1989b) *J. Magn. Reson.*, **85**, 393–399.

Ösapay, K. and Case, D.A. (1991) *J. Am. Chem. Soc.*, **113**, 9436–9444.

Pearson, J.G., Wang, J.-F., Markley, J.L., Le, H. and Oldfield, E. (1995) *J. Am. Chem. Soc.*, **117**, 8823–8829.

Salemme, F., Freer, S., Xuong, N., Alden, R. and Kraut, J. (1973) *J. Biol. Chem.*, **248**, 240–244.

Saunders, M., Wishnia., A. and Kirkwood, J.G. (1957) *J. Am. Chem. Soc.*, **79**, 3289–3290.

Spera, S. and Bax, A. (1991) *J. Am. Chem. Soc.*, **113**, 5490–5492.

Szilágyi, L. (1995) *Prog. NMR Spectrosc.*, **27**, 325–444.

Williamson, M.P., Asakura, T., Nakamura, E. and Demura, M. (1992) *J. Biomol. NMR*, **2**, 83–98.

Wishart, D.S., Sykes, B.D. and Richards, F.M. (1991) *J. Mol. Biol.*, **222**, 311–333.

Wishart, D.S., Sykes, B.D. and Richards, F.M. (1992) *Biochemistry*, **31**, 1647–1651.

Wishart, D.S. and Sykes, B.D. (1994a) *Methods Enzymol.*, **239**, 363–392.

Wishart, D.S. and Sykes, B.D. (1994b) *J. Biomol. NMR*, **4**, 171–180.

Wishart, D.S., Bigam, C.G., Yao, J., Abildgaard, F., Dyson, H.J., Oldfield, E., Markley, J.L. and Sykes, B.D. (1995) *J. Biomol. NMR*, **6**, 135–140.

Yu, L.P. and Smith, G.M. (1990) *Biochemistry*, **29**, 2914–2919.